NeuroImage 230 (2021) 117597

Contents lists available at ScienceDirect

NeuroImage

journal homepage: www.elsevier.com/locate/neuroimage

Registered Report

Effects of Motor Tempo on Frontal Brain Activity: An *f*NIRS Study

Ségolène M.R. Guérin[a], Marion A. Vincent[a], Costas I. Karageorghis[b], Yvonne N. Delevoye-Turrell[a,*]

[a] Univ. Lille, UMR 9193 - SCALab - Sciences Cognitives et Sciences Affectives, F-59000 Lille, France
[b] Brunel University London, Uxbridge, Middlesex, United Kingdom

ARTICLE INFO

Keywords:
Cerebral oxygenation
Prefrontal
Motor timing
Spontaneous motor tempo
Finger tapping

ABSTRACT

People are able to modify the spontaneous pace of their actions to interact with their environment and others. This ability is underpinned by high-level cognitive functions but little is known in regard to the brain areas that underlie such temporal control. A salient practical issue is that current neuroimaging techniques (e.g., EEG, *f*MRI) are extremely sensitive to movement, which renders challenging any investigation of brain activity in the realm of whole-body motor paradigms. Within the last decade, the noninvasive imaging method of functional near-infrared spectroscopy (*f*NIRS) has become the reference tool for experimental motor paradigms due to its tolerance to motion artefacts. In the present study, we used a continuous-wave *f*NIRS system to record the prefrontal and motor hemodynamic responses of 16 participants, while they performed a spatial-tapping task varying in motor complexity and externally-paced tempi (i.e., 300 ms, 500 ms, 1200 ms). To discriminate between physiological noise and cerebral meaningful signals, the physiological data (i.e., heart and respiratory rates) were recorded so that frequency bands of such signals could be regressed from the *f*NIRS data. Particular attention was taken to control the precise position of the optodes in reference to the cranio-cerebral correlates of the NIR channels throughout the experimental session. Results indicated that fast pacing relied on greater activity of the motor areas whereas moving at close-to-spontaneous pace placed a heavier load on posterior prefrontal processes. These results provide new insight concerning the role of frontal cognitive control in modulating the pacing of voluntary motor behaviors.

The coding of time by the brain remains a mystery for the simple reason that there are no time-specific sensory receptors. Initial studies in neuropsychology referred to a normative scale depicted in the form of an internal clock. Conceptualized by Treisman (1963), the internal clock is described as a pacemaker-accumulator model that has become the most popular concept model to date (Droit-Volet and Wearden, 2003). It is composed of three distinct stages in which temporal information about an event is extracted, encoded, and processed. However, the internal clock metaphor was primarily created to fulfill the need of a conceptual framework, and is now challenged by biological and pharmacological research, which suggests that time may be embedded within the neural activity of the cortex (Buhusi and Meck, 2005).

Since the turn of the millennium, neuroscientific studies have indicated that specific brain structures may play a function in time processing; notably the cerebellum and the basal ganglia, with wider networks including the supplementary motor area, the prefrontal cortex, and the posterior parietal cortex (Buhusi and Meck, 2005; Ivry and Spencer, 2004; Rubia and Smith, 2004). However, a major limitation in the literature is the fact that most of the neuroimaging studies have focused on the perception of time, while neglecting the question of motor timing (Bareš et al., 2019; Grahn and Brett, 2007; Jongsma et al., 2007). Although previous findings have indicated that the brain areas dedicated to time perception are similar to those devoted to time production (Rubia and Smith, 2004; Schubotz et al., 2000), due care should be taken in generalizing such results given that these studies were conducted by use of functional magnetic resonance imaging (*f*MRI). It is extremely difficult to execute studies with motor paradigms using *f*MRI, as this technology is highly sensitive to movement artifacts.

Over the last decade, the noninvasive imaging method of functional near-infrared spectroscopy (*f*NIRS) has become the tool of choice for those investigating motor paradigms (Leff et al., 2011). It makes use of the optical proprieties of light in order to evaluate local hemodynamic responses (i.e., increase in blood flow) in a given cortical area. Notably, the brain is one of the body parts in which the metabolic activity is most intense (up to 20% of energy consumption of the body at rest; Attwell et al., 2010; Gusnard and Raichle, 2001) and yet it possesses no reserves of energy. Hence, the brain has developed a large vascular network that can perpetually support its nutritional requirements. The local electrical activity of the neurons (i.e., action potential) engenders an energy cost in oxygen and glucose, that is met by metabolically active cells (i.e., astro-

* Corresponding author.
E-mail address: yvonne.delevoye@univ-lille.fr (Y.N. Delevoye-Turrell).

https://doi.org/10.1016/j.neuroimage.2020.117597
Received 8 July 2020; Received in revised form 13 November 2020; Accepted 17 November 2020
Available online 6 January 2021

cytes; Magistretti et al., 1999). This provides the resources for effective cerebral activity (León-Carrión and León-Domínguez, 2012). *f*NIRS is a neuroimaging technique that provides a means by which to assess such changes in brain metabolism, and thus allows the researcher to infer related neural activity.

Near-infrared spectrum light uses the optical window in which the diffusion of light through biological tissues is the greatest. It is notable that skin, tissue, and bone are mostly transparent to NIR light in the optimal spectrum of 700–900 nm, while oxygenated-hemoglobin (HbO_2) and deoxygenated-hemoglobin (HHb) are stronger absorbers of light. Thus, differences in the absorption spectra of HHb and HbO_2 allow the calculation of the relative changes in hemoglobin concentration (Hb) through the use of the degree of light attenuation at multiple wavelengths (Strangman et al., 2002). Consequently, *f*NIRS can provide specific information on brain oxygenation (i.e., HbO_2), deoxygenation (i.e., HHb), and the total content of hemoglobin (i.e., HbT). In the present study, the *f*NIRS technique was used to measure changes in oxygenation of the brain tissues over the prefrontal and motor areas. This enabled a fuller understanding of the relative contributions of these brain areas to motor timing.

The behavioral task that is most commonly used to study motor timing in experimental psychology is the tapping paradigm (Repp, 2005). Early studies measured the spontaneous tapping speed of the hand—referred to as the *spontaneous motor tempo*—to further understand people's "natural pace" (Fraisse, 1982; Fraisse et al., 1954). Among the general population, this idiosyncratic tempo is subject to considerable interindividual variability (Drake and Baruch, 1995; Fraisse, 1974); nevertheless, spontaneous motor tempo is found to average ~2 Hz (i.e., 500-ms time intervals; McAuley et al., 2006; Moelants, 2002). *f*NIRS has been used in self-paced finger-tapping paradigms (Drenckhahn et al., 2015; Holper et al., 2009; Sato et al., 2007; Wilson et al., 2014). Results have shown that brain hemodynamic responses depend on task complexity, with complex tasks (e.g., bimanual tapping) eliciting significantly larger HbO_2 changes in the premotor area and the primary motor cortex than simple unimanual tapping (Holper et al., 2009). Nonetheless, few studies have used *f*NIRS techniques to ascertain how the brain modulates the spontaneous motor tempo.

Humans live in a constantly changing and evolving environment. Hence, adapted behaviors require individuals to be able to accelerate or decelerate the spontaneous pace of their own motor actions to facilitate smooth interaction with individuals and objects present in their environment (Bryant and Barrett, 2007). Such motor timing abilities are commonly assessed using sensorimotor synchronization tasks. In fact, this approach concerns a form of referential behavior in which an action is temporally coordinated with a predictable external event, the referent (Repp, 2005, p. 969). Sensorimotor synchronization tasks have shown that the ability to adapt the timing of voluntary actions to environmental constraints develops with age as well as experience. For example, babies are unable to alter the speed of their natural behaviors. When required to synchronize self-generated actions to slow auditory stimuli, newborns and 2-month-old babies were reported to be unable to slow down their non-nutritive sucking rate below their spontaneous motor tempo (Bobin-Bègue et al., 2006). Similar results were found in 31/2-year-olds during the synchronization of hand-tapping with slow auditory and visual stimuli (Bobin-Bègue and Provasi, 2008). Bobin-Bègue et al. (2006) suggested that the ability to slow down movements depends on motor inhibition, a process that is a component of high-level cognitive functions. Thus, it would only be acquired later in ontogeny and have functional impact from 8 years and beyond (Williams et al., 1999).

If the ability to modulate motor tempo according to the environmental constraints is underpinned by cognitive functions, it should involve frontal activations. Following this train of thought, Kuboyama et al. (2005; 2004) reported a gradation in cerebral oxygenation of the motor cortex in accord with the frequency at which a finger-tapping task was performed. Larger hemodynamic responses were found for maximal speed tapping compared to slower tapping conditions. However, neither of these studies investigated prefrontal activations as a concomitant of the pace of motor execution.

The main objective of the present study was to examine the cerebral oxygenation of prefrontal and motor areas simultaneously during the execution of visuomotor tasks performed under different time constraints. Three forms of upper-limb movement were used to control for motor complexity and facilitate generalization of the findings: A simple task (i.e., finger-tapping task, discrete movements with a recognizable beginning and end), a task of moderate complexity (i.e., pointing task, serial individual-movements linked together to constitute a whole), and a complex task (i.e., circle drawing task, continuous movements with no recognizable beginning and end; Schmidt et al., 1988). These three sensorimotor synchronization tasks were administered via a computer touchscreen according to three externally-paced tempi: fast pace (i.e., 300 ms), natural pace (i.e., 500 ms), and slow pace (i.e., 1200 ms). A series of self-paced trials (i.e., without an auditory beep) was collected at the start of the experimental session in order to record each participant's spontaneous tempo. The addition of this non-cued condition allowed the research team to control for the effects of auditory cues with reference to brain activations during motor production at a natural pace. To ensure methodological rigor, acquisition and filtering pipelines, as well as raw data, were reported (Leff et al., 2011). To discriminate between physiological noise and cerebral meaningful signals, the physiological data (i.e., heart and respiratory rates) were recorded throughout the experimental session so that frequency bands of such signals could be regressed from the *f*NIRS data. An automatic tracking of the headset was also used to monitor the exact position of the optodes in reference to the cranio-cerebral correlates of the NIR channels.

Motor timing at the spontaneous motor tempo would lead to less prefrontal (i.e., anterior and dorsolateral prefrontal cortices) and motor (i.e., premotor and primary motor cortex) activation when compared to performing the motor task at either fast or slow tempi (H_1). Furthermore, action production at slow tempi would lead to a significantly greater increase in cerebral oxygenation over the prefrontal lobe when compared to task execution at a fast tempo, for which the increase in cerebral oxygenation would involve motor areas (H_2). Similar patterns of activation would be observed regardless of the complexity of the motor task being undertaken (H_3).

2. Methods

2.1. Participants

Healthy adults were recruited for the present study from among the corpus of University of Lille staff and students. Participants were right-handed (assessed by use of the Edinburgh Handedness Inventory; Oldfield, 1971), had normal to corrected-to-normal vision, and did not present motor dysfunction or neurological/psychiatric disorders. A pilot test conducted on two participants confirmed that both hair density and length could induce significant noise in *f*NIRS data (Fig. 1). Ongoing work in our laboratory is targeting potential solutions to address this limitation that pertains to *f*NIRS technology. Nevertheless, for the present study, only male participants with very short haircuts (< 1 cm) or shaven heads were included to avoid hair-related issues (McIntosh et al., 2010; Pringle et al., 1999). Participants were informed of the tasks to be performed and the measurements to be taken at least 48 hr prior to their participation. After reading an information sheet, each participant was invited to provide written informed consent. At this point, demographic data were collected (sex, age, and musical expertise).

The sample size required for the critical statistical test of each research hypothesis was calculated using G*Power (3.1.9.2; see Table 1). For H_1, H_2, and H_3, the *f*NIRS results of Abiru et al. (2016) were used as group parameters. For H_1 and H_2, Tukey post hoc tests were the critical statistical tests. Because a Tukey test is essentially a modified *t* statistic that corrects for multiple comparisons, required sample size was also

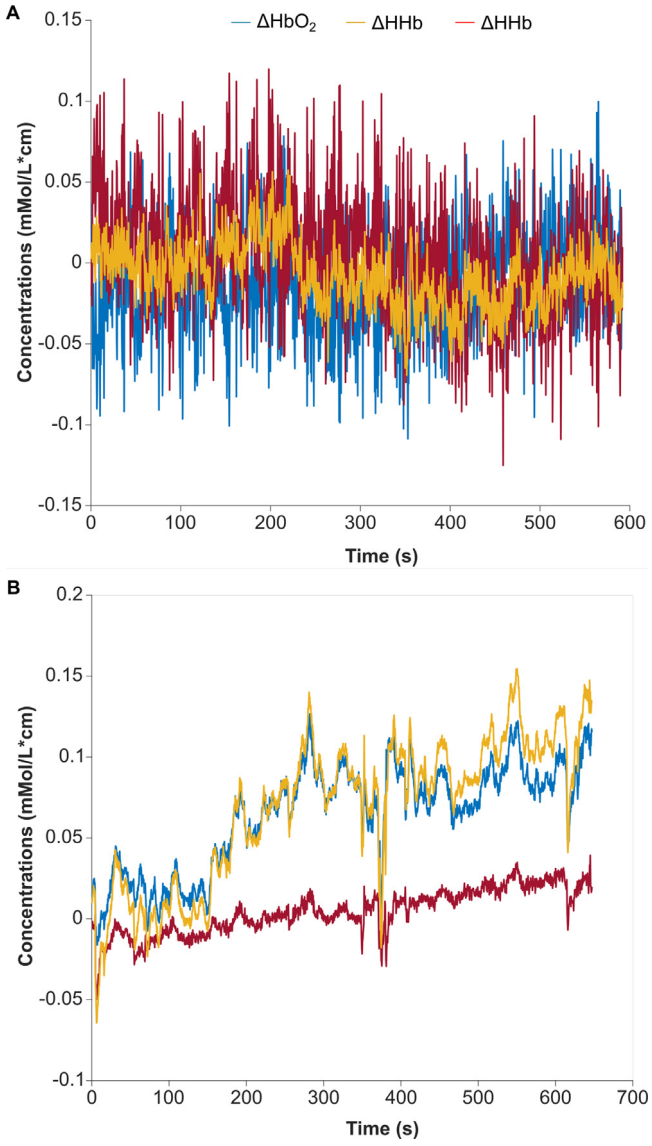

Fig. 1. Raw *f*NIRS data from a participant with hair vs. a participant without hair. *Note.* Raw data for HbO_2, HHb and HbT. Panel A: A typical participant with hair. Pannel B: A typical participant without hair. These data were obtained from a pretest using two participants who performed the finger-tapping task synchronized to an auditory metronome at an interstimuli interval of 500 ms. HbO_2 = oxygenated hemoglobin; HHb = deoxygenated hemoglobin; HbT = total hemoglobin.

computed for paired-samples *t* tests. The power analysis indicated that 15 participants would be required for H_1 ($dz = 0.68$; $\alpha = 0.05$; 1-β = 0.80), and 16 participants for H_2 ($dz = 0.67$; $\alpha = 0.05$; 1-$\beta = 0.80$). For H_3, required sample size was also computed for paired-samples *t* tests. The power analysis indicated that 16 participants would be required ($dz = 0.67$; $\alpha = 0.05$; 1-$\beta = 0.80$). Accordingly, a sample of 16 participants was recruited.

The small telescopes approach was used to determine the smallest effect size of interest (SESOI; i.e., the difference that is considered too small to be meaningful; Simonsohn, 2015) for each hypothesis. Accordingly, the SESOI was set to the effect size that an earlier study would have had 33% power to detect (Lakens et al., 2018). As previously, the *f*NIRS results of Abiru et al. (2016) were used for H_1, H_2, and H_3. The SESOI for each hypothesis is reported in Table 1.

2.2. Experimental Procedure and Tasks

2.2.1. Experimental Procedure

Each participant was administered three visuomotor tasks via a touchscreen on which he used his right index finger, with a closed fist. An *f*NIRS headset was worn by the participant throughout the session. The touchscreen (1915L Elo Touch 19"; Elo Touch Solutions Inc.; Milpitas, California, CA) was placed on a table in front of the participant with the screen oriented at 45°. The participant was seated on a stool, suitably adjusted to her/his height to minimize lower-limb muscular fatigue (assessed by use of the rating-of-fatigue scale; Micklewright et al., 2017) and avoid any extraneous movements during task performance. The stool was fixed in such a way that horizontal rotational movement would be possible. The experimental session took place in a quiet, windowless room that was dimly lit. The lighting is of particular importance given that bright light can affect *f*NIRS signals (Shadgan et al., 2010). The *f*NIRS system (FOIRE-3000/16; Shimadzu, Kyoto, Japan) was placed behind the participant to limit distraction and facilitate the management of the cables. This setup also provided a means by which to minimize the weight of cables on the participant's neck. To verify that this was effective, a self-rated pain scale of was administered. The scale was attached to a 9-point Likert scale, ranging from 1 (*no pain*) to 9 (*unbearable pain*). The participant was required to indicate the degree of pain that he was experiencing in regard to the weight of optodes on the head and neck. This pain scale was presented at the beginning of each block of trials as well as at the end of the experiment, for an overall evaluation of the participant's experience.

2.2.2. Task description

A total of three visuomotor tasks were administered in a counterbalanced order across participants. In the finger-tapping task, the participant was required to tap on a single visual target (dot of 10-mm diameter) located in the center of the touchscreen (Fig. 2, left panel). In the pointing task, six targets (dots of 10-mm diameter) positioned around an invisible circle of 100 mm radius were displayed on the screen. The participant was asked to tap each target, one after the other (Fig. 2, middle panel). In the drawing task, six targets of a similar nature linked together to form a 100-mm circle were displayed on the screen (Fig. 2, right panel). The participant was required to trace the circle and, in so doing, produce a regular and continuous arm movement. In both the pointing and the drawing tasks, the participant was instructed to start with the finger above the top-right target and move counterclockwise. The participant was instructed to maintain accuracy in both temporal

Table 1
Estimated required sample size and critical statistical tests.

Hypotheses	Groups	Measurements	Planned analysis	Critical statistical tests	Required sample size	SESOI
H_1	9	2	RM MANOVA	Contrast 1: 500 ms vs. 300 ms Contrast 2: 500 ms vs. 1200 ms	15	.22
H_2	9	2	RM MANOVA	300 ms vs. 1200 ms	16	.22
H_3	9	2	TOST	Simple vs. moderate task Simple vs. complex task Moderate vs. complex task	16	.22

Note. Statistical power, planned analyses, and critical statistical tests for each research hypothesis. SESOI = smallest effect size of interest (d_z); TOSTs = two one-sided *t* tests.

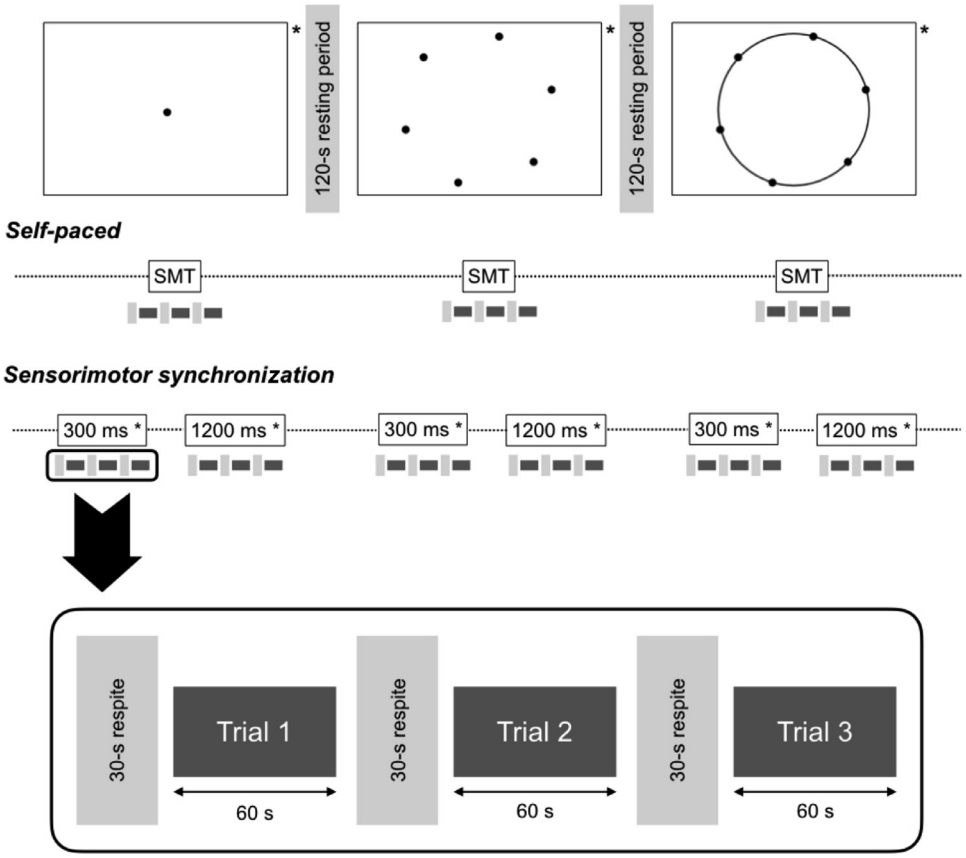

Fig. 2. Diagrammatic representation of the experimental design for the sensorimotor synchronization conditions. *Note.* SMT = spontaneous motor tempo; * = randomization.

and spatial facets of the skill, but to favor temporal accuracy in case the task became too challenging for both to be maintained.

The participant performed the tapping, pointing, and drawing tasks at three predefined tempi that were set by an auditory metronome. The beeps of the metronome had a duration of 80 ms and a sound frequency of 294 Hz. The beeps were generated using Matlab 7.11.0 R2010 software (Mathworks Inc.; Natick, Massachusetts, MA).

The three tempi used in the study were 300 ms (for the fast-tempo trials), 500 ms (for the natural-tempo trials), and 1200 ms (for the slow-tempo trials). For the fast- and slow-tempo trials, this enabled the participant to depart from her/his spontaneous motor tempo but remain within the possible sensorimotor synchronization zone, between 180 ms and 1800 ms (Keele et al., 1985; Mates et al., 1994). These metronome tempi were played to the participant via two Creative SBS 250 desk speakers (Creative Technology; Singapore) positioned either side of the screen.

2.2.3. Experimental design

The experiment was predicated on a block design procedure, characterized by alternating periods of activity and respite to facilitate the acquisition of reliable *f*NIRS signals (Gervain et al., 2011). It has been shown that the best *f*NIRS signal is obtained with a resting period of 30 s prior to stimulation (Obrig et al., 1997). Accordingly, each 60-s trial was preceded by a rest period of 30 s to allow the hemodynamic indices to return to their baseline levels and to optimize the quality of the hemodynamic responses to time-locked body movements.

The participant performed a series of 12 blocks, for a total of 36 trials. In a first series, the participant performed the three visuomotor tasks in a randomized order at a self-paced spontaneous tempo (i.e., executed at a regular and most natural pace). In a second series, he performed the three visuomotor tasks while synchronizing their movements to the metronome. Three blocks of trials were recorded for each task, with the slower, natural, and faster conditions administered in a random order.

Throughout the session, the participant was instructed to leave his left arm hanging by their side in a relaxed manner. The participant was also informed not to speak and to avoid extraneous movements during each *f*NIRS trial. The self-paced trials were systematically administered before the externally-paced trials to avoid cross-contamination (Bove et al., 2009). The total duration of the experimental test period was ~100 min.

2.3. Data acquisition and preprocessing analyses

2.3.1. Behavioral data acquisition and preprocessing

In the tapping and pointing tasks, inter-response intervals (IRIs) were measured as the time interval between the onset of successive taps. In the drawing task, radiuses from the center of the circle to each target were computed first. Taps were defined as the locus that intersected the participant's finger and each radius. Before conducting the main analyses, the time series were checked in order to detect and remove the IRIs greater than twice the ISI of the given block of trials. These trials were referred to as "temporal omissions" and were not included in the statistical analyses.

An IRI error (IRI_{error}) was computed as the percentage of absolute difference between an IRI and its reference ISI for a given time interval *t* (Eq. 1).

$$IRI_{error(t)} = (|IRI_t - ISI|)/ISI \times 100 \quad (1)$$

The mean IRI_{error} measurement within a trial indicated the accuracy of time interval production (i.e., behavioral tempo-accurary; Repp, 2005).

For each time interval *t*, a spatial error was computed (pixels), as the difference between the center of the visual target and the location

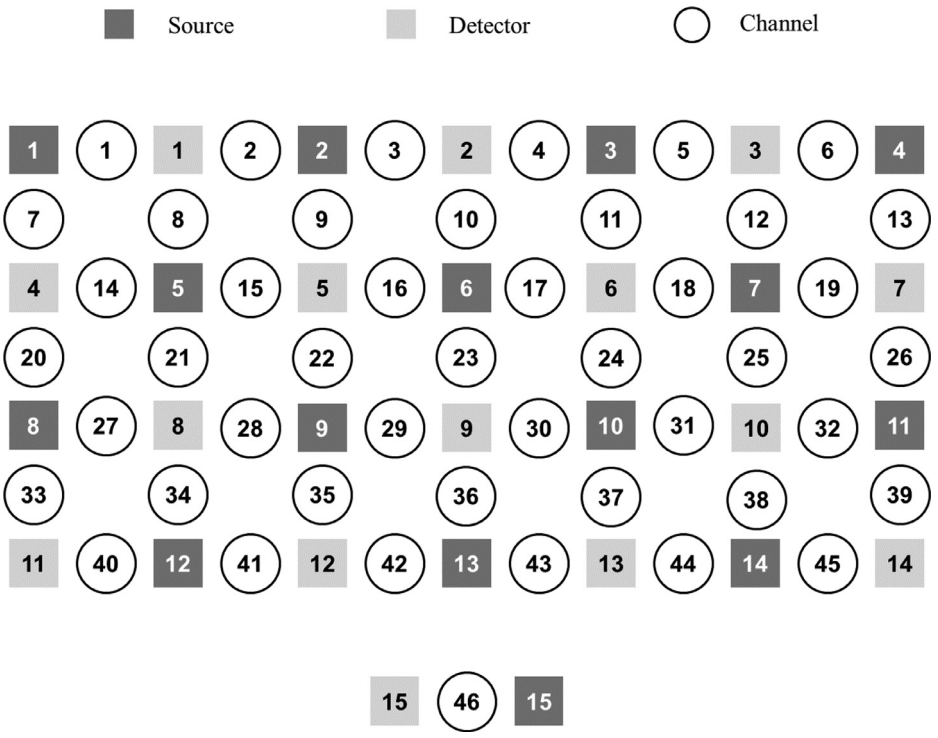

Fig. 3. Diagrammatic representation of the sources, detectors, and channel layout. *Note.* Adjacent sources and detectors were 3 cm apart.

of the participant's forefinger. The mean pointing error within a trial was used as an indicator of behavioral-spatial accuracy (Dione and Delevoye-Turrell, 2015).

2.3.2. fNIRS data acquisition

Data were collected using a continuous-wave *f*NIRS system operating at three near-infrared wavelenghts (780 nm, 805 nm, and 830 nm) and monitored by the associated LabNIRS software. This *f*NIRS system offers 32 optodes divided into 16 light sources (multicomponent glass bundle fibers) and 16 detectors (multi-alkali photomultipliers detectors). The sampling frequency was set at 2.27 Hz (i.e., temporal resolution of 440 ms).

The brain regions of interest were the prefrontal cortex (anterior and dorsolateral prefrontal cortices; Brodmann's areas 9 and 10) and motor cortex (premotor and primary motor cortices; Brodmann's areas 4 and 6; Homan et al., 1987; Okamoto et al., 2004). Thus, a 45-channel (28 optodes, 45 source-detector couples) configuration was applied in order to cover these cortices over both brain hemispheres (Fig. 3). One additional channel was applied to the occipital cortex (Brodmann's area 18) as a means of providing "negative control" (i.e., control an area of the brain not expected to be influenced by the experimental manipulations). The optodes were attached to a 32-optode headset with a 3-cm source-detector distance, giving a depth of analysis from 0.5–2.0 cm. The headset was placed on each participant's head in accord with the International 10–20 system guidelines for standard electrode positions (Jasper, 1958). As a result, the Cz optode was located at the midway point between the nasion and inion.

System calibration was performed through an automatic adjustment using LabNIRS to adapt the internal parameters of the *f*NIRS device (e.g., gain, amount of light to emit) to the head morphology and the hair-type characteristics of each participant. Differences in the absorption of HbO_2 and HHb provided the means to measure the differences in the hemoglobin concentration (μmol/L). These differences were computed in real time using Eqs. 2 and 3 (Baker et al., 2014, generated by LabNIRS from the modified Beer-Lambert law):

$$HbO_2 = (-1.4887) \times Abs[780\,nm] + 0.5970 \times Abs[805\,nm] + 1.4847 \times Abs[830\,nm] \quad (2)$$

$$HHb = 1.8545 \times Abs[780\,nm] + (-0.2394) \times Abs[805\,nm] + (-1.0947) \times Abs[830\,nm] \quad (3)$$

The total hemoglobin (HbT) will then be established through a summation of HbO_2 and HHb (Eq. 4):

$$HbT = HbO_2 + HHb \quad (4)$$

2.3.3. Preprocessing of fNIRS Data

Data (HHb, HbO_2, and HbT) were first filtered to eliminate mechanical artifacts (quick baseline shifts of the signal waveform characterized by sharp and steep edges) and physiological noise (heart and respiratory rates). This enabled the research team to keep only the physiological hemodynamic signals X (HHb, HbO_2, and HbT), which show slow variations over time (Pinti et al., 2019). The precise preprocessing pipeline was defined in accord with the shape of the data, as there is presently no consensus in the *f*NIRS literature regarding filtering methods (Pinti et al., 2019).

For each trial i, a baseline $B_{X,i}$ and a plateau $P_{X,i}$ were defined as the mean values of X upon a 5-s time window starting 10 s before the trial onset and upon the last 5 s of the trial, respectively, for similar calculations, see (Mandrick, 2013). Then, the variations $\Delta_{X,i}$ of a trial were given relative to its baseline (i.e., by subtracting $B_{X,i}$ to $P_{X,i}$), to be free from possible offsets across trials and linear trends of the signal over time. The mean $\bar{\Delta}_{X,n}$ was computed over each block n, for each channel, in each condition, for similar calculations, see (Derosière et al., 2014; Mandrick et al., 2013). Finally, the mean variations in HbO_2, HHb, and HbT were given for two channel clusters defined according to the two regions of interest: $\bar{\Delta}_{X,\,prefrontal}$ and $\bar{\Delta}_{X,\,motor}$.

2.3.4. Controlling for noisy signals

Data contamination caused by movement and physiological artifacts in *f*NIRS is an important consideration with regard to reaping the full potential of the technique for real-life applications (Jahani et al., 2018).

In the present study, we applied tracking methods to identify sources of noisy data. The synchronization of the different systems was controlled by means of Matlab algorithms. The central command computer controlled for motor tasks; it sent triggers to the other apparatus—including the *f*NIRS system—to segment the times of onsets and offsets in an automated manner. A similar triggering system was used in our previous studies (e.g., Blampain et al., 2018), which revealed a synchronization error of ~35 ms. Visual tags were used to identify the beginning and end of each trial, with specific tags for each trial type.

2.3.4.1. Cardiorespiratory monitoring. By use of the Fourier transform method, both heart and respiratory rates can be identified in the *f*NIRS frequency spectrum. The ability to identify these two frequency components serves to ensure the validity of *f*NIRS measures. In terms of frequency, the neurophysiological detail in the *f*NIRS signals is lower than that of both heart and respiratory rates ~2 Hz and ~0.3 Hz, respectively (Pinti et al., 2019). Thus, these physiological components were filtered out, which restricted any potential contamination from the raw *f*NIRS signal.

Cardiorespiratory monitoring was done using the MP150 Biopac system (Biopac Systems, Goleta, CA), complemented with two dedicated add-on wearable devices. To avoid recording movement artifacts, heart rate (HR) data (Hz) were captured by use of an ECG Bionomadix module (wireless transmitter and RPEC-R amplifier) and low-pass filtered to 1 Hz. Two disposable patch electrodes were placed on the participant's right and left clavicles. Respiration rate (Hz) was recorded using the TSD201 respiratory effort transducer, which was wired to the RSP100C amplifier. This respiratory belt was placed around the chest wall, at the level of the sternum. Sampling frequency was set to 250 Hz. Data acquisition was facilitated by the AcqKnowledge software that is included in the MP system.

2.3.4.2. Headset position tracker. Data were collected using three Oqus 5+ cameras (Qualisys MoCap, Göteborg, Sweden) to control for any shift in the headset. The spatial positions were measured in real time using three spherical passive markers taped to the participant's right temple and headset (with the use of one and two markers, respectively). The distance between the temple marker and each of the two headset markers was computed (in cm) based on Cartesian coordinates (i.e., *x*, *y*, and *z*). The Real-Time Motion Capture (RTMocap) Matlab toolbox (Lewkowicz and Delevoye-Turrell, 2016) was used to interpolate any missing data. The spatial accuracy of the system is 0.5 mm for each dimension of 3D space.

To verify the occurrence of a *f*NIRS helmet shift, a deformation calculation of the area of the planar triangle connecting the 3D markers was used. This was referred to as the *mesh area*. Notably, if the 3D markers remain in the same place with respect to each other, the mesh area remains constant. On the other hand, if the two markers of the headset move relative to the reference marker (i.e., temple marker), the mesh area is modified.

The mesh area between the three markers M_i, with $i \in \{0;1;2\}$, at a given moment in time $t \in [1;d]$, with d defined as the acquisition duration, was computed using a scalar product (Eq. 5), equal to twice the mesh area.

$$\overrightarrow{M_0M_1}(t) \cdot \overrightarrow{M_0M_2}(t) = \begin{pmatrix} x_1(t) - x_0(t) \\ y_1(t) - y_0(t) \\ z_1(t) - z_0(t) \end{pmatrix} \cdot \begin{pmatrix} x_2(t) - x_0(t) \\ y_2(t) - y_0(t) \\ z_2(t) - z_0(t) \end{pmatrix} \quad (5)$$

If $\overrightarrow{M_0M_1} \cdot \overrightarrow{M_0M_2}$ remained constant over time with an acceptable error threshold, an absence of deformation of the mesh was considered and indicative of an absence of headset shift. In the present study, the error threshold ϵ was set to 10 mm, which corresponds to the degree of spatial resolution of the *f*NIRS optical imaging technique (Quaresima and Ferrari, 2016). The variation Δ_{mesh} of the $\overrightarrow{M_0M_1} \cdot \overrightarrow{M_0M_2}$ value was computed. If this value exceeded 15%, which corresponds with ϵ, the participant's data from that block of trials as well as from subsequent blocks were removed for the purposes of statistical analysis, as it was difficult to determine the exact sources of the recorded hemodynamic signals.

2.4. Statistical analyses

2.4.1. Data eligible for analysis

HbT reflects the overall changes in corpuscular blood volume of the sampling volume. Because HbT is a summation of HbO_2 and HHb changes (see Eq. 4), it was not statistically analyzed. The behavioral data were analyzed and reported in a supplementary online file. HHb and HbO_2 data were analyzed only from those blocks of trials characterized by (a) at least 70% level of behavioral accuracy, and (b) an absence of headset shift. A participant's entire data set was removed if > 25% of his data were ineligible and any excluded participants were replaced.

Given that an absence of cerebral activation can be informative, both activated and non-activated channels were taken into consideration. In addition, the ratio of activated to non-activated channels (i.e., if $B_{X,i}$ and $P_{X,i}$ are significantly different) was reported for each trial. Only HbO_2 data were used to support or refute hypotheses. However, HHb data were also statistically analyzed to improve specificity of *f*NIRS signals, as recommended in the *f*NIRS literature (e.g., Leff et al., 2011; Tachtsidis and Scholkmann, 2016). The alpha level was set at $p < .05$ for all statistical analyses.

2.4.2. Analyses undertaken

2.4.2.1. Classic null-hypothesis significance tests. The dependent variables, $\bar{\Delta}_{HbO_2}$ and $\bar{\Delta}_{HHb}$ for each of the two regions of interest were analyzed. To examine H_1 and H_2, a oneway RM MANOVA (Externally-Paced Tempo [300 ms, 500 ms, 1200 ms]) was applied. Normality was checked using the Shapiro–Wilk test; if violated, the data were normalized using a transformation that was contingent on data distribution curves (e.g., log10). Where Mauchly's tests indicated violations of the sphericity assumption, Greenhouse–Geisser corrections were applied. Tukey post hoc tests were used where necessary (see Table 1).

2.4.2.2. Equivalence tests. It is not acceptable to use nonsignificance of the interaction term from an ANOVA to claim the absence of an interaction effect (Cribbie et al., 2016). Consequently, to confirm that similar effects of externally-paced tempo were observed regardless of the task complexity (H_3), two one-sided tests (TOSTs) were used (Lakens et al., 2018). In this procedure—referred to as *equivalence testing*—the SESOI is used to test whether an effect is sufficiently close to zero to reject the presence of a meaningful difference (Harms and Lakens, 2018, p. 385). The results of both *t* tests needed to reach significance in order for equivalence to be claimed. To date, the TOST procedure has only been used in a oneway ANOVA design (Campbell and Lakens, 2019), and has yet to be extended to interaction effects. Accordingly, TOST were computed on the *change score* (i.e., difference between the 300-ms and 1200-ms tempo trials) between (a) the simple and moderate tasks, (b) the simple and complex tasks, and (c) the moderate and complex tasks. TOSTs were computed using the TOSTER R package for paired-samples *t* tests (Lakens, 2017).

2.4.3. Outcome-neutral validation tests

The *f*NIRS technique is rather new in the field of human brain sciences and so defining a positive control provides many challenges. Consequently, a negative control condition was included by placing an additional channel over the occipital brain region (Broadmann's area 18). This region is involved primarily in visual perception and so its activation should remain fairly consistent across pacing conditions and motor tasks. Accordingly, TOSTs (Lakens et al., 2018) were computed for paired-samples *t* tests between the baseline $B_{X,occipital}$ and the plateau $P_{X,occipital}$ for each block of trials. Statistically nonsignificant differences

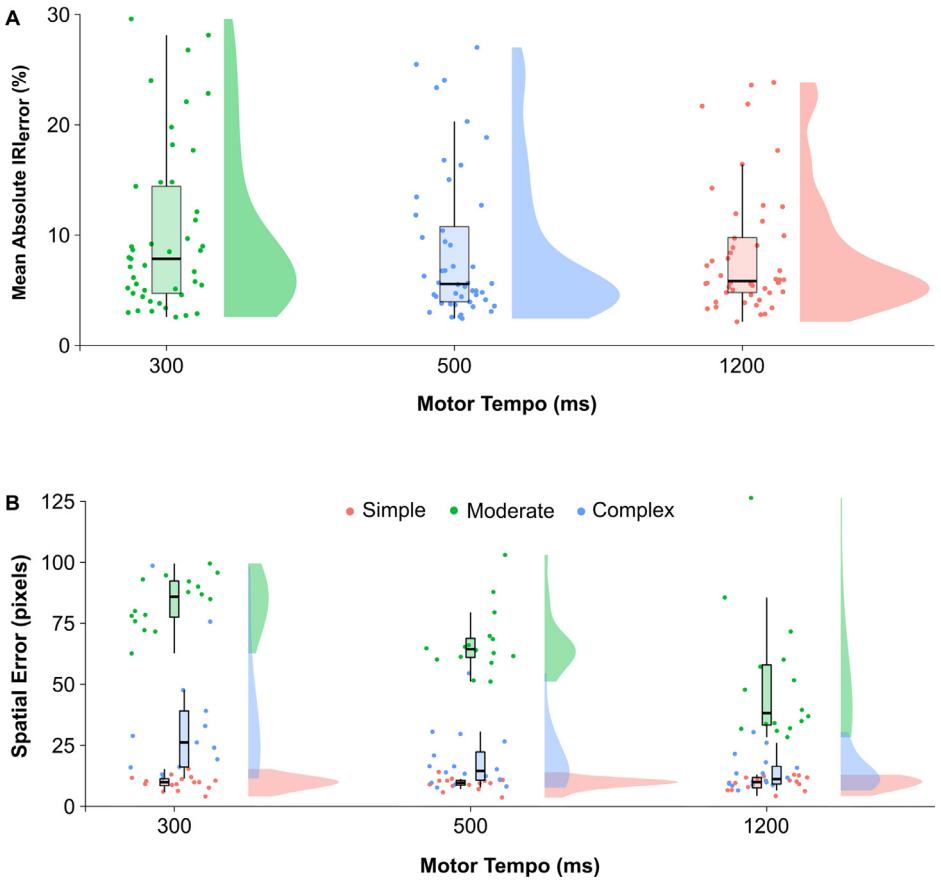

Fig. 4. Behavioral results for each experimental condition. *Note.* Panel A: Mean IRI_{error}. Box plots and density distributions are displayed for each designated motor tempo. Each dot represents an individual participant. IRI = inter-response interval. Panel B: Mean spatial errors. Box plots and density distributions are displayed for each designated motor tempo and level of task complexity. Each dot represents an individual participant.

provided a means by which to confirm that observed prefrontal and motor activations are related to the modulation of motor tempo. If differences were detected over the occipital brain region, the delta activation was removed from all other delta values.

3. Results

3.1. Behavioral data

3.1.1. Time-interval accuracy

The RM ANOVA showed a significant main effect of motor tempo, $F(2, 24) = 6.88$, $p = 0.004$, $\eta_p^2 = 0.36$, with more IRI_{error} in the 300 ms ISI ($M = 10.79$, $SD = 3.39$) than in the 500 ms ($M = 8.54$, $SD = 2.84$) and 1200 ms ISI conditions ($M = 8.23$, $SD = 2.74$; Fig. 4). The main effect of task complexity was also significant, $F(2, 24) = 77.86$, $p < 0.001$, $\eta_p^2 = 0.87$, with a smaller IRI_{error} in the simple ($M = 4.51$, $SD = 1.62$) and moderate tasks ($M = 5.89$, $SD = 1.59$) compared to the complex task ($M = 17.17$, $SD = 5.75$). The Motor Tempo × Task Complexity interaction was nonsignificant ($p = 0.117$). Overall, the results indicated that participants made more timing errors under a fast externally-paced tempo and when the task was complex.

3.1.2. Spatial accuracy

The RM ANOVA showed a significant main effect of motor tempo, $F(2, 24) = 20.38$, $p < 0.001$, $\eta_p^2 = 0.63$, with the spatial errors decreasing from the 300 ms ISI ($M = 42.75$, $SD = 13.04$) to the 1200 ms ISI ($M = 24.58$, $SD = 11.86$). The main effect of task complexity was also significant, $F(2, 24) = 78.88$, $p < .001$, $\eta_p^2 = .87$, with fewer spatial errors in the simple task ($M = 9.56$, $SD = 2.61$) than in the complex one ($M = 22.34$, $SD = 14.98$), and in the complex than in the moderate task ($M = 100.73$, $SD = 16.53$). The Motor Tempo × Task Complexity interaction was significant, $F(4, 48) = 8.54$, $p = 0.001$, $\eta_p^2 = .42$. This indicated that spatial errors were smaller in the simple task than in the complex one in the 300 ms ($p < 0.001$) and the 500 ms ISI conditions ($p < 0.001$); however, the spatial errors were similar in the simple and complex tasks in the 1200 ms ISI condition (Fig. 4). Overall, the results showed that participants made more spatial errors when required to move through space quickly.

3.2. Headset position tracker

The absolute variation Δ_{mesh} did not exceed the 15% threshold for any of our participants ($M = 0.91$, $SD = 0.87$). The maximum percentage change observed was 3.13%. Overall, the data confirmed the absence of an *f*NIRS helmet shift, meaning that the 3D markers held the same relative positions throughout the experimental trials.

3.3. fNIRS Data

3.3.1. Preprocessing

Given that our *f*NIRS system does not provide access to raw intensities, preprocessing was performed directly on Δ_{HbO_2} and Δ_{HHb} concentrations. This was achieved using Matlab, with both personal code and algorithm adapted from the Matlab-based toolbox Homer2 (Massachusetts General Hospital, Boston, MA, USA). The preprocessing steps are detailed in Fig. 5.

The *f*NIRS literature details several filtering methods (Herold et al., 2018; Hocke et al., 2018; Pinti et al., 2019) and a hybrid filtering of

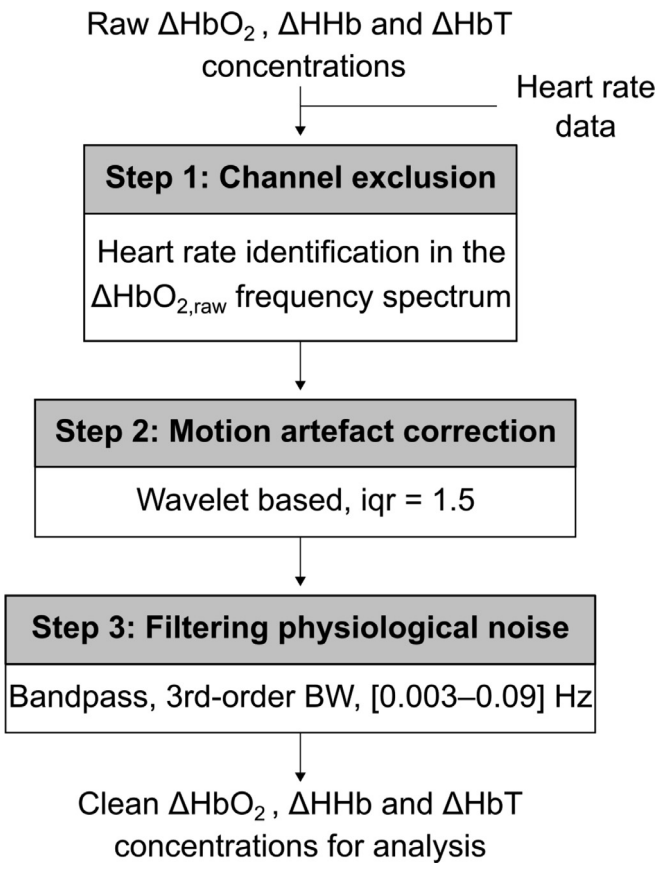

Fig. 5. Preprocessing pipeline of *f*NIRS data. *Note.* HbO_2 = oxygenated-hemoglobin; HHb = deoxygenated-hemoglobin; iqr = interquartile range; BW = Butterworth filter.

the *f*NIRS time-series was applied in the present study (cf. Jahani et al., 2018). First, the wavelet-based method was used to perform motion-artefact correction, as it appeared to apply particularly well to our dataset, and has been shown to be relatively efficient (Hocke et al., 2018). Second, *f*NIRS data were bandpass filtered to remove physiological noise that was concomitant to the task-induced hemodynamic activity.

3.3.1.1. Channel exclusion criterion. The first mandatory step was to control for the optical-coupling quality of the acquired *f*NIRS data (Orihuela-Espina et al., 2010; Pinti et al., 2019; Scholkmann et al., 2017). Optical coupling is characterized by the presence of heart-beat oscillations within the *f*NIRS signals. A frequency inspection of the raw *f*NIRS time series enabled the exclusion of channels with a poor optical coupling (i.e., an absence of HR in the power spectrum of *f*NIRS signals). Only Δ_{HbO_2} raw data were analyzed, as HbO_2 is more sensitive to cardiac oscillation than HHb (Pinti et al., 2019). A two-step process was used to check the 45 channels for each participant: First, applying power-spectrum density (PSD; i.e., frequency domain) to the raw data, the frequency corresponding to maximal peak in the 50-160 beat-per-minute (bpm) range was detected. Second, to guarantee that the identified frequency was indeed the HR frequency, it was compared to the HR measurements provided by the Biopac system, with a tolerance threshold of 7 bpm.

Following the aforementioned steps, three participants were excluded due to an absence of heart beat oscillations in the *f*NIRS signal across all channels pertaining to at least one region of interest. In addition, the channels for which we failed to identify cardiac-frequency component for all participants were excluded from subsequent statistical analyses. Overall, 34.8% of channels were rejected on this basis. Examples of both acceptable and excluded channels are shown in Fig. 6.

3.3.1.2. Motion correction: wavelet filtering. *f*NIRS signals recorded during body movements are prone to motion artefacts. Accordingly, motion correction was performed to remove motion-induced sharp and fast skips from the raw *f*NIRS time series (see Fig. 7). To this end, the wavelet-based smoothing method described by Molavi and Dumont (2012) and implemented in Homer2 (hmrMotionCorrect_Wavelet function, interquartile-range [iqr] = 1.5) was adapted to process concentrations rather than of optical densities. The motion-corrected data were visually inspected to ensure that the selected iqr value was well suited to the present dataset.

3.3.1.3. Bandpass filtering of physiological noise. Hemodynamic responses elicited by a cognitive process are jeopardized by physiological processes that are not directly linked to the task being undertaken (Scholkmann et al., 2014; Tachtsidis et al., 2004). To minimize the effects of spontaneous hemodynamic activity—HR (~1 Hz), breathing rate (~0.3 Hz), Mayer waves (i.e., arterial pressure oscillations; ~0.1 Hz), and very low frequency oscillations (VLF, < 0.04 Hz)—motion-corrected *f*NIRS signals were bandpass filtered.

A third-order Butterworth filter was applied to extract relevant frequencies (Fig. 7) The high cut-off frequency (lowpass) was set to 0.09 Hz to reject both cardiac and breathing rates and parts of Mayer oscillations. The highpass was set at 0.003 Hz to preserve the stimulation protocol frequency (1 / (task + rest) = 0.01 Hz) without attenuation (0 dB flat frequency band of the filter). The 2nd and 3rd harmonics that contained important information were also preserved (Pinti et al., 2019). Fig. 7 summarizes the steps taken in the hybrid filtering process.

3.3.2. Outcome-neutral validation tests

The TOST procedure (SESOI = 0.8) showed that both *t* tests were significant, $t_{upper}(15) = 4.48$, $p < 0.001$, $t_{lower}(15) = 1.92$, $p = 0.037$. Thus, equivalence was established, confirming that occipital activations remained similar across tempo conditions and levels of task complexity.

3.3.3. Oxygenated hemoglobin

To detect non-activated channels, $\bar{\Delta}_{HbO_2}$ was tested against zero by means of a one-sided *t* test within each of the 45 channels. To account for multiple comparisons, Bonferroni corrections were applied (.05 ÷ 45; $\alpha = 0.001$). Results showed that all $\bar{\Delta}_{HbO_2}$ were significantly different from zero. Collectively, the results indicate that 100% of the channels were activated.

3.3.3.1. Motor channels. The RM ANOVA showed a significant main effect of motor tempo, $F(2, 30) = 5.77$, $p = 0.007$, $\eta_p^2 = 0.28$, with a smaller $\bar{\Delta}_{HbO_2}$ in the 1200 ms ISI ($M = 1.85$, $SD = 6.52$) than in the 300 ms ISI ($M = 4.94$, $SD = 7.60$, $d_z = 0.43$) and the 500 ms ISI conditions ($M = 4.23$, $SD = 7.26$, $d_z = 0.34$; Fig. 8). Note that the effect size of both contrasts was larger than the required SESOI (see Table 1), which indicated that the effects were sufficiently strong to be considered meaningful.

The TOST procedure (SESOI = 0.62; Miyai et al., 2001) computed on the change score between the simple and moderate tasks showed that both *t* tests were significant, $t_{upper}(15) = 2.97$, $p = 0.005$, $t_{lower}(15) = 1.97$, $p = 0.034$. However, neither of the TOST procedures computed on the change score between (a) the simple and complex tasks ($p_{upper} = 0.003$, $p_{lower} = 0.159$), and (b) the moderate and complex tasks ($p_{upper} = 0.002$, $p_{lower} = 0.183$) reached significance. Overall, the results confirmed similar effects of motor tempo across the simple and moderate tasks over the motor areas (see Table 2).

3.3.3.2. Prefrontal Channels. The RM ANOVA showed a significant main effect of motor tempo, $F(2, 30) = 3.93$, $p = 0.030$, $\eta_p^2 = 0.21$, with a larger $\bar{\Delta}_{HbO_2}$ in the 500 ms ISI ($M = 3.75$, $SD = 6.51$) than in

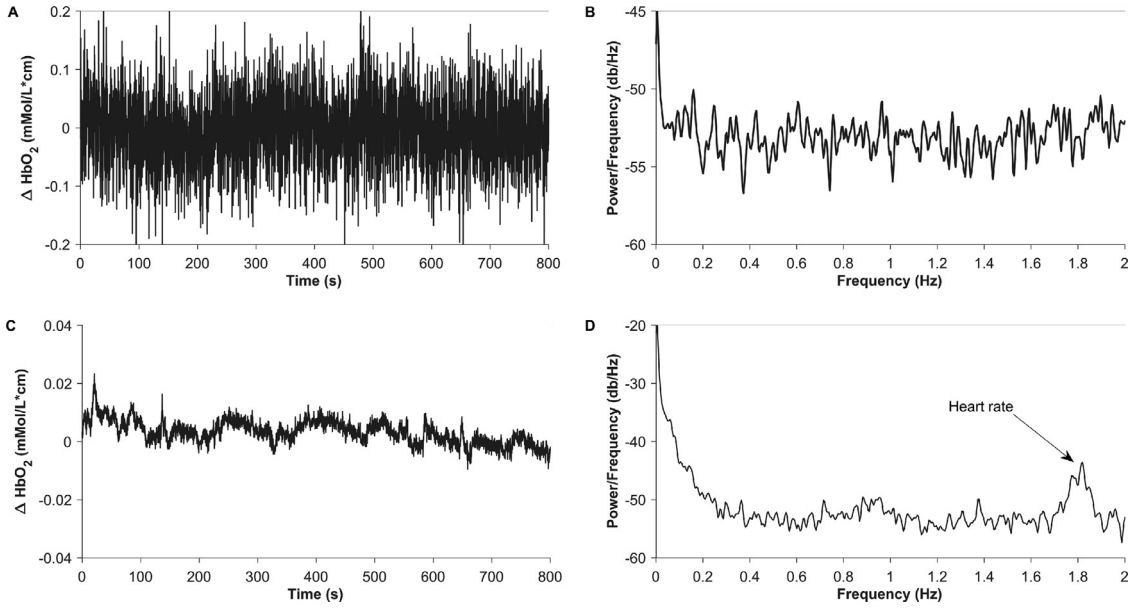

Fig. 6. Raw data and power-spectrum density of two levels of signal-to-noise ratio *Note.* Samples of Δ_{HbO_2} recorded on channel 17 for two participants (left), and their respective power spectrum (right). Heart rate frequency was not identified in the power-spectrum density for a time-series with a poor signal-to-noise ratio (SNR; top right), but present with high SNR (bottom right).

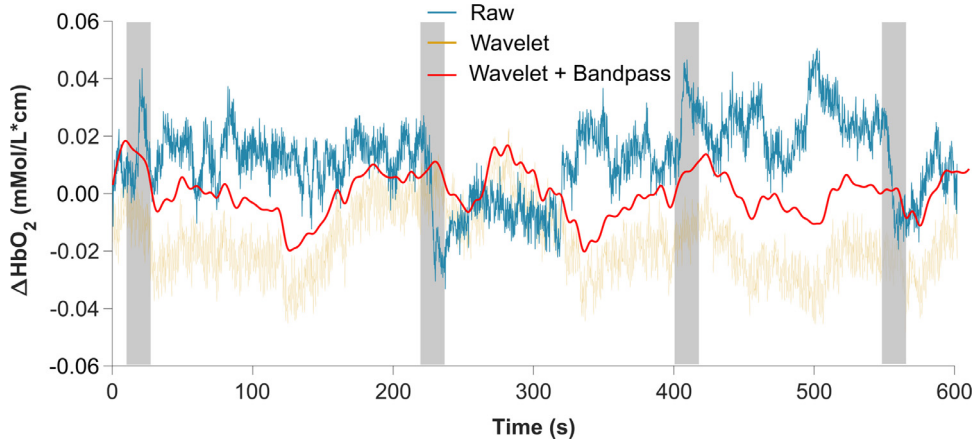

Fig. 7. Filtering of the *f*NIRS signal. *Note.* Example of the filtering of motion artefact (wavelet based, brown) and physiological noise (bandpass, red) fromΔ_{HbO_2} data (channel 33, blue). Areas highlighted in gray represent motion-kind and baseline shift artefacts.

Table 2
Oxyhemoglobin anddeoxyhemoglobin change scores over the motor and prefrontal regions of interest.

Regions of Interest	Oxyhemoglobin		Deoxyhemoglobin	
	M	*SD*	*M*	*SD*
Motor				
Simple	0.97	8.28	0.15	1.99
Moderate	2.22	9.33	0.36	2.15
Complex	5.54	7.65	0.46	3.09
Prefrontal				
Simple	0.51	6.61	0.29	2.81
Moderate	0.75	8.06	0.04	1.50
Complex	2.45	8.24	0.40	3.45

Note. Means and standard deviations for oxyhemoglobin and deoxyhemoglobin change scores (i.e., $\bar{\Delta}_{HbO_2}$ 300 ms - $\bar{\Delta}_{HbO_2}$ 1200 ms) for each motor task. A positive value indicates higher activations for 300 ms vs. 1200 ms.

the 1200 ms condition (M = 1.06, SD = 5.52, d_z = 0.44; Fig. 8). Note that the effect size of the contrast was larger than the required SESOI, which indicated that the effect was sufficiently strong to be considered meaningful.

The TOST procedure (SESOI = 0.62) computed on the change score between the simple and moderate tasks showed that both t tests were significant, $t_{upper}(15) = 2.56$, $p = 0.011$, $t_{lower}(15) = 2.38$, $p = 0.015$. However, neither of the TOST procedures computed on the change score between (a) the simple and complex tasks (p_{upper} =.007, $p_{lower} = 0.072$), and (b) the moderate and complex tasks (p_{upper} =.007, $p_{lower} = 0.069$) were significant. Overall, these results indicated similar effects of motor tempo across the simple and moderate complexity tasks over the prefrontal areas (see Table 2).

3.3.4. *Deoxygenated hemoglobin*

3.3.4.1. Motor channels. The RM ANOVA ran on the $\bar{\Delta}_{HHb}$ was non-significant (p =.749). The TOST procedure (SESOI = 0.62) computed on the change score between the simple and moderate tasks showed that both t tests were significant, $t_{upper}(15) = 2.20$, $p = 0.022$, $t_{lower}(15) = 2.75$, $p = 0.008$. However, neither of the TOST procedures computed on the change score between (a) the simple and complex tasks ($p_{upper} = 0.008$, $p_{lower} = 0.062$), and (b) the moderate and complex tasks ($p_{upper} = 0.007$, $p_{lower} = 0.073$) were significant. Overall, these results indicated

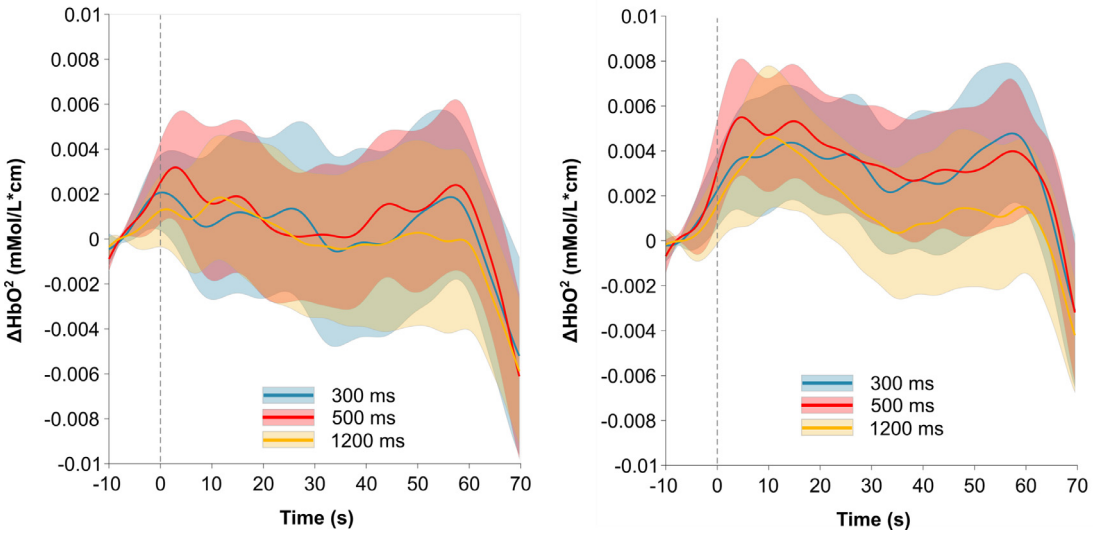

Fig. 8. *f*NIRS data for each experimental condition. *Note.* Panel A: Mean $\bar{\Delta}_{HbO_2}$ and $\bar{\Delta}_{HHb}$ for each motor tempo in the prefrontal channels. 95% confidence intervals are represented by the shaded area that surrounds each trace. Panel B: Mean $\bar{\Delta}_{HbO_2}$ and $\bar{\Delta}_{HHb}$ for each motor tempo in the motor channels. 95% confidence intervals are represented by the shaded area that surrounds each trace.

similar effects of motor tempo across the simple and moderate complexity tasks over the motor areas (see Table 2).

3.3.4.2. Prefrontal channels. The RM ANOVA performed on the $\bar{\Delta}_{HHb}$ was nonsignificant (p =.529). The TOST procedure (SESOI = 0.62) computed on the change score between the simple and moderate tasks showed that both t tests were significant, $t_{upper}(15) = 2.92$, $p = 0.005$, $t_{lower}(15) = 2.03$, $p = 0.030$. The TOST procedure computed on the change score between the moderate and complex tasks showed that both t tests were significant, $t_{upper}(15) = 2.63$, $p = 0.011$, $t_{lower}(15) = 1.82$, $p = 0.047$. However, the TOST procedure computed for the change score between the simple and complex tasks was nonsignificant ($p_{upper} = 0.007$, $p_{lower} = 0.071$). Overall, these results indicated similar effects of motor tempo over the prefrontal area across the simple and moderate complexity tasks, and in the moderate and complex tasks (see Table 2).

3.4. Exploratory analyses

Through visual inspection, we noticed that HbO_2 began to increase just prior to initiation of the task (see Fig. 8). It is notable that the epoch used to compute $B_{HbO_2,i}$ (i.e., from 5 s to 10 s before the trial onset) coincided with when HbO_2 had already started to increase. To make $B_{HbO_2,i}$ more representative of the baseline level, additional analyses were applied for which $B_{HbO_2,i}$ was taken from 20 s to 10 s prior to trial onset. These findings are presented in the paragraphs that follow.

The RM ANOVA performed on the motor channels showed a significant main effect of motor tempo, $F(2, 30) = 7.04$, $p = 0.003$, $\eta_p^2 = 0.32$, with a smaller $\bar{\Delta}_{HbO_2}$ in the 1200 ms ($M = 3.06$, $SD = 5.21$) than in the 300 ms ISI ($M = 6.74$, $SD = 6.65$, $d_z = 0.59$) and the 500 ms ISI conditions ($M = 5.94$, $SD = 6.05$, $d_z = 0.50$). Note that the effect size of both contrasts was larger than the required SESOI, which indicated that the effects were strong enough to be considered meaningful. None of the TOST procedures computed on the change score between (a) the simple and moderate tasks ($p_{upper} = 0.001$, $p_{lower} = 0.093$), (b) the simple and complex tasks ($p_{upper} = 0.005$, $p_{lower} = 0.097$), and (c) the moderate and complex tasks ($p_{upper} = 0.009$, $p_{lower} = 0.056$) were significant. Overall, these results indicate dissimilar effects of motor tempo over the motor region. A oneway RM ANOVA (Task Complexity [simple, moderate, complex]) was also computed but found to be nonsignificant (p = 0.966).

The RM ANOVA performed on the prefrontal channels showed a significant main effect of motor tempo, $F(2, 30) = 6.11$, $p = 0.006$, $\eta_p^2 = 0.29$, with a larger $\bar{\Delta}\_HbO_2$ in the 500 ms ISI ($M = 5.81$, $SD = 5.23$) than in the 1200 ms conditions ($M = 2.83$, $SD = 5.14$, $d_z = 0.57$). Note that the effect size of the contrast was larger than the required SESOI, which indicated that the effect was sufficiently strong to be considered meaningful. The TOST procedure computed on the change score between the simple and moderate tasks showed that both t tests were significant, $t_{upper}(15) = 2.97$, $p = 0.005$, $t_{lower}(15) = 1.97$, $p = 0.034$. The same effects were observed between the simple and complex tasks, $t_{upper}(15) = 2.64$, $p = 0.011$, $t_{lower}(15) = 1.82$, $p = 0.047$, and between the moderate and complex tasks, $t_{upper}(15) = 2.38$, $p = 0.017$, $t_{lower}(15) = 2.08$, $p = 0.030$. Overall, these results confirmed similar effects of motor tempo over the prefrontal region, regardless of level of task complexity.

4. Discussion

The main purpose of the present study was to investigate frontal brain activity under conditions of different speeds of motor execution. Three forms of upper-limb movement were used as sensorimotor-synchronization tasks and performed at fast (i.e., 300 ms), natural (i.e., 500 ms), and slow paces (i.e., 1200 ms). H_1 was not supported as performing the tasks at spontaneous motor tempo did not yield less prefrontal and motor activation than moving faster or slower. Action production at fast tempi led to greater motor oxygenation compared to action production at slow tempi, which replicated the previously-reported effect of larger increases in HbO_2 over the motor cortex when a movement is executed at a fast pace (Kuboyama et al., 2005; 2004). However, moving at slow tempi did not lead to greater increases in cerebral oxygenation over the prefrontal lobe when compared to the faster tempo. Accordingly, H_2 is partially verified. Equivalence tests on task complexity were significant for the two finger-tapping tasks only, and not for the continuous-drawing task. Hence, H_3 was also only partially verified.

4.1. Cerebral responses

Collectively, the present findings demonstrated the ability of *f*NIRS to dissociate the involvement of different cognitive mechanisms as a function of task constraints. The first important result is that the motor areas were activated to a greater degree when producing actions at fast vs. slow tempi. In addition, TOST tests and descriptive data confirmed

that this pattern of results was potentiated in the complex task (i.e., circle drawing; see Table 2). These findings are congruent with the *dynamic systems* approach of motor timing, in which behavior is described as the emergent product of a self-organizing, multicomponent system evolving over time (Perone and Simmering, 2017, p. 44). Indeed, behavioral studies have reported that the production of fast movements is dependent on dynamic processes (Huys et al., 2008). In this respect, the temporal organization of movements performed at 300 ms of ISI would emerge from the regularities of body-dynamics (e.g., mass, length, velocity; Zelaznik et al., 2002). Hence, there would be less cognitive control applied upon motor execution (Lemoine, 2007). The findings of the present study extend the behavioral literature by providing evidence that fast movement production is underpinned predominantly by central and non-reflective motor processes.

The second important result is that performing a task at a slow pace did not induce larger prefrontal hemodynamic responses when compared to performing at a fast pace. Explanation for this unexpected finding lies with a measurement issue. Being limited to 47 channels by our *f*NIRS system, we were not able to optimally cover the prefrontal areas of the brain: A unique row of channels is accounted for on the dorsolateral cortex. Therefore, it is possible that the ability to modulate motor tempo according to environmental constraints is underpinned by cognitive functions that might be pinpointed further forward in the brain.

By way of illustration, the medial prefrontal cortex has been proposed to control the adaptive responses to context, location, and events (Di Pellegrino et al., 2007; Euston et al., 2012), and could play a central role in performing a motor task at a slow tempo. However, it would not have been recorded with the current *f*NIRS measurement configuration. Even further frontal is the orbitofrontal cortex, which is implicated in response inhibition (Evans et al., 2004; Horn et al., 2003). In futures studies, there will be a clear need for more accurate contrasts of the activation loci evident across different prefrontal areas. This will facilitate delineation of the frontal-cognitive processes that underlie the ability to execute slow movements.

4.2. Spontaneous motor tempo

It is notable that motor timing at the spontaneous motor tempo led to greater prefrontal activation. It could be that the recorded activation does not originate from the dorsolateral cortex but from the supplementary motor area (SMA), which is located close to the recorded channels. Using the fOLD toolbox (*f*NIRS Optodes Location Decider; Morais et al., 2018), we found that the recorded prefrontal activation had a ~25% likelihood of having originated from the SMA. Relative to other neuroimaging techniques (e.g., EEG), the *f*NIRS spatial resolution is quite good; nonetheless, the measured activity is localized within the brain with an error of ~1 cm (Herold et al., 2018). Therefore, the *f*NIRS technique may not afford sufficient fidelity to distinguish dorsolateral prefrontal cortex activity from SMA activity.

Macar et al. (2006) proposed that, as part of the striato-cortical pathway, the SMA plays a key role in time processing. In previous studies with *f*MRI, the pre-SMA was found to be more activated when participants were directed to selectively attend to time in perceptual-timing tasks (Coull, 2004; Coull et al., 2004). It is noteworthy that the SMA was more involved for tempi close to spontaneous pace (i.e., 540 ms ISI) than for slower tempi (i.e., 1080 ms ISI; Coull et al., 2012). There is similarity with the present findings, which show significantly greater prefrontal activation in spontaneous vs. slow-pace movement using analogous time intervals. In addition, patients with SMA lesions have been reported to be impaired in rhythm-reproduction tasks in the absence of auditory cues; nonetheless, they were perfectly able to produce rhythms when auditory pacing was provided (Halsband et al., 1993). Accordingly, the SMA may be more strenuously involved in internally-generated movements rather than in the external guidance of timed movements (Rao et al., 1997). The increase of prefrontal activation identified in the present study was occasioned by motor execution at a spontaneous pace (i.e., the instinctive speed associated with self-initiated action). As scientific knowledge stands, the cerebral correlates of motor production at a spontaneous motor tempo are unclear. A plausible hypothesis emanating from the present findings is that the SMA, and more specifically the pre-SMA, which has projections to and from the prefrontal cortex (Kim et al., 2010), serves a pivotal role in motor timing at (close-to-) spontaneous pace.

4.3. Behavioral outcome

An original contribution of the present study concerns the three forms of upper-limb movement that were used to control for motor complexity. The behavioral results indicated that participants were less accurate in their time-interval production when they performed the complex (i.e., circle-drawing task) vs. the easier tasks (i.e., finger-tapping and pointing tasks). The same pattern of results was found using *f*NIRS: Identical effects of externally-paced tempo were observed for both the prefrontal and motor areas between the simple and moderate tasks, but not between these tasks and their complex counterpart. Accordingly, it seems that the performance of a timing task is more laborious in continuous motion than in discrete actions.

Discrete actions are characterized by a recognizable beginning and end; thus, they are much easier to synchronize with external events than continuous movements, for which there is no recognizable beginning and end. In the present study, motor activation could have been more salient when motor-timing control was challenging. Interestingly, the complementary analysis (performed on the first peak of hemodynamic activation) showed that an externally-paced tempo elicited similar effects regardless of motor complexity in the prefrontal cortex. Conversely, the three equivalence tests failed to reach significance in terms of the activation of motor areas. This finding suggests that the three upper-limb movements required different planning and execution strategies, but similar degrees of cognitive control for performance outcome.

4.4. Strengths and limitations

The combination of *f*NIRS measurement with physiological indices has been advocated in recent years and referred to as *systemic-physiology-augmented fNIRS* (SPA-*f*NIRS; Scholkmann et al., 2017). The *f*NIRS technique enables the researcher to draw inferences about neural activity through the assessment of cerebral blood oxygenation. However, given that cardiac contractions contribute significantly to cerebral oxygen supply, the frequency of these contractions must be identified in the *f*NIRS signal of interest. Without such identification, the recorded signal might only contains non-physiological fluctuations. In the present study, the validity of the recorded *f*NIRS signal was verified through detailed observation of the relevant physiological information derived from the *f*NIRS channels (i.e., HR and respiratory frequency; see Figure 6). Collectively, the preprocessing data confirmed that the application of *f*NIRS to motor paradigms is a scientifically legitimate endeavor. Furthermore, we illustrated the importance of using physiological measurements to identify and select the channels of interest. Therefore, it is evident that SPA-*f*NIRS should be used in a systematic manner to verify that *f*NIRS data are sound, even in experimental paradigms that do not involve movement-based tasks.

The methodological advancement evident in the present study entails a rigorous procedure for the acquisition and processing of *f*NIRS data in the realm of whole-body movement. First, a 3D reconstruction of the headset position on the participant's head was used. This control is of paramount importance, as it enables the researcher to ascertain the precise location of the recorded *f*NIRS signal throughout an experimental session. In the current study, no *f*NIRS headset shifts were detected (on average, < 1% of variation during the experimental session), even in tasks requiring moving through space (e.g., the circle-drawing trials). Second, channel selection was undertaken to ascertain whether cardiac

frequency was visible in the *f*NIRS signals (Pinti et al., 2019). Through this preprocessing method, only those channels with meaningful inputs were kept in the regions of interest. Finally, a hybrid filter technique that was applied proved effective in removing instrumental noise, motion-related artefacts, and physiological oscillations (for a review of noise source in *f*NIRS signals, see Herold et al., 2018) without overfiltering the signal, which seems to be a common phenomenon in the NIRS literature.

In terms of limitations of the present study, the three types of upper-limb movements that were chosen are simple laboratory-based tasks that have limited ecological validity. In addition, it is possible that the natural-pace condition did not best reflect the spontaneous motor tempo of a few participants. A condition developed from prior measurement of each participant's spontaneous motor tempo could have enhanced internal validity somewhat. The decision to select only participants with very short hair (< 1 cm) is also acknowledged as a minor limitation. Given that only male participants were recruited, we cannot readily generalize the findings to both sexes.

4.5. Future directions

The present work serves to illustrate the technical challenges related to using whole-brain *f*NIRS in movement paradigms. Nonetheless, a few recent articles providing recommendations for *f*NIRS application are beginning to emerge in the scientific literature (e.g., Herold et al., 2018; Perrey, 2014; Pinti et al., 2019). It is hoped that researchers will take up the gauntlet of investigating cognitive processes underlying time production and use realistic, whole-body movements in so doing. Such explorations will represent a meaningful contribution to the knowledge base of cognitive neuroscience by providing a broader picture of how the brain modulates motor timing.

Future research might also address the role of the brains functional connectivity in the adaptation of motor timing (see Vergotte et al., 2018; 2017). The assessment of *f*NIRS connectivity between the prefrontal cortex and motor areas holds potential to provide valuable insights on the cerebral dynamics underlying time production. This form of rich detail is obfuscated when researchers focus solely upon the activation pattern of one or two regions of interest.

From a methodological point of view, future research will need to tackle the dissociation of prefrontal from SMA activations. With this aim in mind, it will be appropriate to take anatomical specificity into account through tailoring the placement of *f*NIRS channels to the brain morphology of each participant; this *neuronavigational approach* will substantially increase the accurate identification of the brain areas of interest (Herold et al., 2018). Close attention will also need to be given to the choice of experimental motor tasks, as different brain patterns can be observed as a function of the discrete vs. continuous dimension of motor skill execution. Researchers might use naturalistic movements that mirror those used in everyday life, such as walking or cycling.

4.6. Conclusions and recommendations

When examined collectively, the present findings indicate that motor tasks performed either at a fast or slow tempo will result in differences in brain activation. *f*NIRS can be used to gain a fuller understanding of the brain dynamics involved in the modulation of motor tempo. Fast pacing relies on greater activity of the motor areas whereas moving at close-to-spontaneous pace places a heavier load on posterior prefrontal processes. These findings are consistent with the notion that two timing modes exist (Huys et al., 2008; Madison and Delignieres, 2009); they confirm that the execution of fast movements (i.e., faster than the spontaneous motor tempo) depend on dynamic systems from which bodily movements emerge (Zelaznik et al., 2002). The effects of spontaneous motor pacing on prefrontal brain activity are possibly the result of the SMA involvement for motor execution at natural pace. With *f*NIRS technology, the scientific community has a means by which to unravel the mystery surrounding how the brain controls time production.

Declaration of Competing Interest

The authors have no competing financial interests to declare.

Credit authorship contribution statement

Ségolène M.R. Guérin: Conceptualization, Methodology, Writing - original draft, Investigation, Visualization, Writing - review & editing. **Marion A. Vincent:** Formal analysis, Investigation, Visualization, Writing - review & editing. **Costas I. Karageorghis:** Methodology, Writing - original draft, Writing - review & editing. **Yvonne N. Delevoye-Turrell:** Conceptualization, Methodology, Writing - original draft, Writing - review & editing.

References

Abiru, M., Sakai, H., Sawada, Y., Yamane, H., 2016. The effect of the challenging two handed rhythm tapping task to DLPFC activation. Asian J. Occup. Therapy 12 (1), 75–83. doi:10.11596/asiajot.12.75.

Attwell, D., Buchan, A.M., Charpak, S., Lauritzen, M., MacVicar, B.A., Newman, E.A., 2010. Glial and neuronal control of brain blood flow. Nature 468 (7321), 232–243. doi:10.1038/nature09613.

Baker, W.B., Parthasarathy, A.B., Busch, D.R., Mesquita, R.C., Greenberg, J.H., Yodh, A., 2014. Modified Beer-Lambert law for blood flow. Biomed. Opt. Express 5 (11), 4053–4075. doi:10.1364/BOE.5.004053.

Bareš, M., Apps, R., Avanzino, L., Breska, A., D'Angelo, E., Filip, P., Gerwig, M., Ivry, R.B., Lawrenson, C.L., Louis, E.D., Lusk, N.A., Manto, M., Meck, W.H., Mitoma, H., Petter, E.A., 2019. Consensus paper: Decoding the contributions of the cerebellum as a time machine. From neurons to clinical applications. The Cerebellum 18 (2), 266–286. doi:10.1007/s12311-018-0979-5.

Blampain, J., Ott, L., Delevoye-Turrell, Y.N., 2018. Seeing action simulation as it unfolds: The implicit effects of action scenes on muscle contraction evidenced through the use of a grip-force sensor. Neuropsychologia 114, 231–242. doi:10.1016/j.neuropsychologia.2018.04.026.

Bobin-Bègue, A., Provasi, J., 2008. Régulation rythmique avant 4 ans : effet d'un tempo auditif sur le tempo moteur. L'Année Psychologique 108, 631–658. Rhythmic regulation before 4 years: Effect of an auditory tempo on the motor tempo

Bobin-Bègue, A., Provasi, J., Marks, A., Pouthas, V., 2006. Influence of auditory tempo on the endogenous rhythm of non-nutritive sucking. Eur. Rev. Appl. Psychol. 56 (4), 239–245. doi:10.1016/j.erap.2005.09.006.

Bove, M., Tacchino, A., Pelosin, E., Moisello, C., Abbruzzese, G., Ghilardi, M.F., 2009. Spontaneous movement tempo is influenced by observation of rhythmical actions. Brain Res. Bull. 80 (3), 122–127. doi:10.1016/j.brainresbull.2009.04.008.

Bryant, G.A., Barrett, H.C., 2007. Recognizing intentions in infant-directed speech: evidence for universals. Psychol. Sci. 18 (8), 746–751. doi:10.1111/j.1467-9280.2007.01970.x.

Buhusi, C.V., Meck, W.H., 2005. What makes us tick? Functional and neural mechanisms of interval timing. Nat. Rev. Neurosci. 6 (10), 755–765. doi:10.1038/nrn1764.

Campbell, H., Lakens, D., Can we disregard the whole model? Omnibus non-inferiority testing for R^2 in multivariable linear regression and η^2 in ANOVA. Br. J. Math. Stat. Psychol.

Coull, J.T., 2004. *f*MRI studies of temporal attention: allocating attention within, or towards, time. Cogn. Brain Res. 21 (2), 216–226. doi:10.1016/j.cogbrainres.2004.02.011.

Coull, J.T., Hwang, H.J., Leyton, M., Dagher, A., 2012. Dopamine precursor depletion impairs timing in healthy volunteers by attenuating activity in putamen and supplementary motor area. J. Neurosci. 32 (47), 16704–16715. doi:10.1523/JNEUROSCI.1258-12.2012.

Coull, J.T., Vidal, F., Nazarian, B., Macar, F., 2004. Functional anatomy of the attentional modulation of time estimation. Science 303 (5663), 1506–1508. doi:10.1126/science.1091573.

Cribbie, R.A., Ragoonanan, C., Counsell, A., 2016. Testing for negligible interaction: a coherent and robust approach. Br. J. Math. Stat. Psychol. 69 (2), 159–174. doi:10.1111/bmsp.12066.

Derosière, G., Alexandre, F., Bourdillon, N., Mandrick, K., Ward, T.E., Perrey, S., 2014. Similar scaling of contralateral and ipsilateral cortical responses during graded unimanual force generation. NeuroImage 85, 471–477. doi:10.1016/j.neuroimage.2013.02.006.

Di Pellegrino, G., Ciaramelli, E., Làdavas, E., 2007. The regulation of cognitive control following rostral anterior cingulate cortex lesion in humans. J. Cogn. Neurosci. 19 (2), 275–286. doi:10.1162/jocn.2007.19.2.275.

Dione, M., Delevoye-Turrell, Y., 2015. Testing the co-existence of two timing strategies for motor control in a unique task: The synchronisation spatial-tapping task. Hum. Mov. Sci. 43, 45–60. doi:10.1016/j.humov.2015.06.009.

Drake, C., Baruch, C., 1995. De la mesure de la sensibilité temporelle aux modèles d'organisation temporelle : hypothèses et donnÉes sur l'acquisition des capacités temporelles auditives. L'année Psychologique 95 (4), 555–569.

doi:10.3406/psy.1995.28855. From measurement of temporal sensitivity to temporal organization models: Hypotheses and data on the acquisition of temporal auditory abilities

Drenckhahn, C., Koch, S.P., Dümmler, J., Kohl-Bareis, M., Steinbrink, J., Dreier, J.P., 2015. A validation study of the use of near-infrared spectroscopy imaging in primary and secondary motor areas of the human brain. Epilepsy Behav. 49, 118–125. doi:10.1016/j.yebeh.2015.04.006.

Droit-Volet, S., Wearden, J., 2003. Les modȩles d'horloge interne en psychologie du temps. L'année Psychologique 103 (4), 617–654. doi:10.3406/psy.2003.29656. Internal clock models in the psychology of time

Euston, D.R., Gruber, A.J., McNaughton, B.L., 2012. The role of medial prefrontal cortex in memory and decision making. Neuron 76 (6), 1057–1070. doi:10.1016/j.neuron.2012.12.002.

Evans, D.W., Lewis, M.D., Iobst, E., 2004. The role of the orbitofrontal cortex in normally developing compulsive-like behaviors and obsessive–compulsive disorder. Brain Cogn. 55 (1), 220–234. doi:10.1016/S0278-2626(03)00274-4.

Fraisse, P., 1974. Psychologie du Rythme. Presses Universitaires de France. Psychology of the rhythm

Fraisse, P., 1982. Rhythm and Tempo, 1. Academic Press, pp. 149–180.

Fraisse, P., Chambron, H., Oléron, G., 1954. Note sur la constance et l'évolution génétique du tempo spontané moteur. Enfance 7 (1), 25–34. doi:10.3406/enfan.1954.1311. The constancy and genetic evolution of spontaneous motor rhythm

Gervain, J., Mehler, J., Werker, J.F., Nelson, C.A., Csibra, G., Lloyd-Fox, S., Shukla, M., Aslin, R.N., 2011. Near-infrared spectroscopy: A report from the McDonnell infant methodology consortium. Dev. Cogn. Neurosci. 1 (1), 22–46. doi:10.1016/j.dcn.2010.07.004.

Grahn, J.A., Brett, M., 2007. Rhythm and beat perception in motor areas of the brain. J. Cogn. Neurosci. 19 (5), 893–906. doi:10.1162/jocn.2007.19.5.893.

Gusnard, D.A., Raichle, M.E., 2001. Searching for a baseline: functional imaging and the resting human brain. Nat. Rev. Neurosci. 2 (10), 685–694. doi:10.1038/35094500.

Halsband, U., Ito, N., Tanji, J., Freund, H.-J., 1993. The role of premotor cortex and the supplementary motor area in the temporal control of movement in man. Brain 116 (1), 243–266. doi:10.1093/brain/116.1.243.

Harms, C., Lakens, D., 2018. Making 'null effects' informative: Statistical techniques and inferential frameworks. J. Clin. Transl. Res. 3 (Suppl. 2), 382–393. doi:10.18053/jctres.03.2017S2.007.

Herold, F., Wiegel, P., Scholkmann, F., Müller, N.G., 2018. Applications of functional near-infrared spectroscopy (*f*NIRS) neuroimaging in exercise–cognition science: a systematic, methodology-focused review. J. Clin. Med. 7 (12). doi:10.3390/jcm7120466. Article e466

Hocke, L.M., Oni, I.K., Duszynski, C.C., Corrigan, A.V., Frederick, B.d., Dunn, J.F., 2018. Automated processing of *f*NIRS data: a visual guide to the pitfalls and consequences. Algorithms 11 (5). doi:10.3390/a11050067. Article e67

Holper, L., Biallas, M., Wolf, M., 2009. Task complexity relates to activation of cortical motor areas during uni-and bimanual performance: a functional NIRS study. NeuroImage 46 (4), 1105–1113. doi:10.1016/j.neuroimage.2009.03.027.

Homan, R.W., Herman, J., Purdy, P., 1987. Cerebral location of international 10–20 system electrode placement. Electroencephalogr. Clin. Neurophysiol.y 66 (4), 376–382. doi:10.1016/0013-4694(87)90206-9.

Horn, N., Dolan, M., Elliott, R., Deakin, J.F., Woodruff, P., 2003. Response inhibition and impulsivity: an *f*MRI study. Neuropsychologia 41 (14), 1959–1966. doi:10.1016/S0028-3932(03)00077-0.

Huys, R., Studenka, B.E., Rheaume, N.L., Zelaznik, H.N., Jirsa, V.K., 2008. Distinct timing mechanisms produce discrete and continuous movements. PLOS Comput. Biol. 4. doi:10.1371/journal.pcbi.1000061. Article e1000061

Ivry, R.B., Spencer, R.M., 2004. The neural representation of time. Curr. Opin. Neurobiol. 14 (2), 225–232. doi:10.1016/j.conb.2004.03.013.

Jahani, S., Setarehdan, S.K., Boas, D.A., Yücel, M.A., 2018. Motion artifact detection and correction in functional near-infrared spectroscopy: a new hybrid method based on spline interpolation method and Savitzky–Golay filtering. Neurophotonics 5 (1), 1–11. doi:10.1117/1.NPh.5.1.015003.

Jasper, H.H., 1958. Report of the committee on methods of clinical examination in electroencephalography. Electroencephalogr. Clin. Neurophysiol. 10, 370–375. doi:10.1016/0013-4694(58)90053-1.

Jongsma, M.L., Meeuwissen, E., Vos, P.G., Maes, R., 2007. Rhythm perception: speeding up or slowing down affects different subcomponents of the ERP P3 complex. Biol. Psychol. 75 (3), 219–228. doi:10.1016/j.biopsycho.2007.02.003.

Keele, S.W., Pokorny, R.A., Corcos, D.M., Ivry, R., 1985. Do perception and motor production share common timing mechanisms: a correlational analysis. Acta Psychol. 60 (2–3), 173–191. doi:10.1016/0001-6918(85)90054-X.

Kim, J.-H., Lee, J.-M., Jo, H.J., Kim, S.H., Lee, J.H., Kim, S.T., Seo, S.W., Cox, R.W., Na, D.L., Kim, S.I., et al., 2010. Defining functional SMA and pre-SMA subregions in human MFC using resting state *f*MRI: Functional connectivity-based parcellation method. NeuroImage 49 (3), 2375–2386. doi:10.1016/j.neuroimage.2009.10.016.

Kuboyama, N., Nabetani, T., Shibuya, K., Machida, K., Ogaki, T., 2005. Relationship between cerebral activity and movement frequency of maximal finger tapping. J. Physiol. Anthropol. Appl. Hum. Sci. 24 (3), 201–208. doi:10.2114/jpa.24.201.

Kuboyama, N., Nabetani, T., Shibuya, K.-i., Machida, K., Ogaki, T., 2004. The effect of maximal finger tapping on cerebral activation. J. Physiol. Anthropol. Appl. Hum. Sci. 23 (4), 105–110. doi:10.2114/jpa.23.105.

Lakens, D., 2017. Equivalence tests: a practical primer for *t*tests, correlations, and meta-analyses. Soc. Psychol. Person. Sci. 8 (4), 355–362. doi:10.1177/1948550617697177.

Lakens, D., Scheel, A.M., Isager, P.M., 2018. Equivalence testing for psychological research: a tutorial. Adv. Methods Pract. Psychol.Sci. 1 (2), 259–269. doi:10.1177/2515245918770963.

Leff, D.R., Orihuela-Espina, F., Elwell, C.E., Athanasiou, T., Delpy, D.T., Darzi, A.W., Yang, G.-Z., 2011. Assessment of the cerebral cortex during motor task behaviours in adults: a systematic review of functional near infrared spectroscopy (*f*NIRS) studies. NeuroImage 54 (4), 2922–2936. doi:10.1016/j.neuroimage.2010.10.058.

Lemoine, L., 2007. Implication des processus de timing évènementiels et émergents dans la gestion des aspects temporels du mouvement. Montpellier 1 Ph.D. thesis.

León-Carrión, J., León-Domínguez, U., 2012. Functional near-infrared spectroscopy (*f*NIRS): Principles and neuroscientific applications. InTech, pp. 47–74.

Lewkowicz, D., Delevoye-Turrell, Y., 2016. Real-time motion capture toolbox (RTMocap): an open-source code for recording 3-D motion kinematics to study action–effect anticipations during motor and social interactions. Behav. Res. Methods 48 (1), 366–380. doi:10.3758/s13428-015-0580-5.

Macar, F., Coull, J., Vidal, F., 2006. The supplementary motor area in motor and perceptual time processing: *f*MRI studies. Cogn. Process. 7 (2), 89–94. doi:10.1007/s10339-005-0025-7.

Madison, G., Delignieres, D., 2009. Auditory feedback affects the long-range correlation of isochronous serial interval production: support for a closed-loop or memory model of timing. Exp. Brain Res. 193 (4), 519–527. doi:10.1007/s00221-008-1652-x.

Magistretti, P.J., Pellerin, L., Rothman, D.L., Shulman, R.G., 1999. Energy on demand. Science 283 (5401), 496–497. doi:10.1126/science.283.5401.496.

Mandrick, K., 2013. Application de la spectroscopie proche infrarouge dans la discrimination de la charge de travail. Doctoral dissertation, Montpellier 1.

Mandrick, K., Derosiere, G., Dray, G., Coulon, D., Micallef, J.-P., Perrey, S., 2013. Prefrontal cortex activity during motor tasks with additional mental load requiring attentional demand: a near-infrared spectroscopy study. Neurosci. Res. 76 (3), 156–162. doi:10.1016/j.neures.2013.04.006.

Mates, J., Müller, U., Radil, T., Pöppel, E., 1994. Temporal integration in sensorimotor synchronization. J. Cogn. Neurosci. 6 (4), 332–340. doi:10.1162/jocn.1994.6.4.332.

McAuley, J.D., Jones, M.R., Holub, S., Johnston, H.M., Miller, N.S., 2006. The time of our lives: life span development of timing and event tracking. J. Exp. Psychol.: Gen. 135 (3), 348–367. doi:10.1037/0096-3445.135.3.34.

McIntosh, M.A., Shahani, U., Boulton, R.G., McCulloch, D.L., 2010. Absolute quantification of oxygenated hemoglobin within the visual cortex with functional near infrared spectroscopy (*f*NIRS). Investig. Ophthalmol. Vis. Sci. 51 (9), 4856–4860. doi:10.1167/iovs.09-4940.

Micklewright, D., Gibson, A.S.C., Gladwell, V., Al Salman, A., 2017. Development and validity of the rating-of-fatigue scale. Sports Med. 47 (11), 2375–2393. doi:10.1007/s40279-017-0711-5.

Miyai, I., Tanabe, H.C., Sase, I., Eda, H., Oda, I., Konishi, I., Tsunazawa, Y., Suzuki, T., Yanagida, T., Kubota, K., 2001. Cortical mapping of gait in humans: A near-infrared spectroscopic topography study. NeuroImage 14 (5), 1186–1192. doi:10.1006/nimg.2001.0905.

Moelants, D., 2002. Preferred tempo reconsidered. In: Nair, D.G., Large, E.W., Steinberg, F., Kelso, J.A.S., Stevens, K., Burnham, D., Renwick, J. (Eds.), Proceedings of the 7th International Conference on Music Perception and Cognition, pp. 1–4.

Molavi, B., Dumont, G.A., 2012. Wavelet-based motion artifact removal for functional near-infrared spectroscopy. Physiol. Meas. 33 (2), 259–270. doi:10.1088/0967-3334/33/2/259.

Morais, G.A.Z., Balardin, J.B., Sato, J.R., 2018. fNIRS optodes' location decider (fOLD): a toolbox for probe arrangement guided by brain regions-of-interest. Sci. Rep. 8 (1), 1–11. doi:10.1038/s41598-018-21716-z.

Obrig, H., Hirth, C., Junge-Hülsing, J.G., Döge, C., Wenzel, R., Wolf, T., Dirnagl, U., Villringer, A., 1997. Length of Resting Period Between Stimulation Cycles Modulates Hemodynamic Response to a Motor Stimulus. Springer, pp. 471–480.

Okamoto, M., Dan, H., Sakamoto, K., Takeo, K., Shimizu, K., Kohno, S., Oda, I., Isobe, S., Suzuki, T., Kohyama, K., Dan, I., 2004. Three-dimensional probabilistic anatomical cranio-cerebral correlation via the international 10–20 system oriented for transcranial functional brain mapping. NeuroImage 21 (1), 99–111. doi:10.1016/j.neuroimage.2003.08.026.

Oldfield, R.C., 1971. The assessment and analysis of handedness: The Edinburgh inventory. Neuropsychologia 9 (1), 97–113.

Orihuela-Espina, F., Leff, D.R., James, D.R., Darzi, A.W., Yang, G.-Z., 2010. Quality control and assurance in functional near infrared spectroscopy (*f*NIRS) experimentation. Phys. Med. Biol. 55 (13), 3701. doi:10.1088/0031-9155/55/13/009.

Perone, S., Simmering, V.R., 2017. Applications of Dynamic Systems Theory to Cognition and Development: New Frontiers, 52. Academic Press, pp. 43–80.

Perrey, S., 2014. Possibilities for examining the neural control of gait in humans with *f*NIRS. Front. Physiol. 5. doi:10.3389/fphys.2014.00204. Article e204

Pinti, P., Scholkmann, F., Hamilton, A., Burgess, P., Tachtsidis, I., 2019. Current status and issues regarding pre-processing of *f*nirs neuroimaging data: An investigation of diverse signal filtering methods within a general linear model framework. Front. Hum. Neurosci. 12. doi:10.3389/fnhum.2018.00505. Article e505

Pringle, J., Roberts, C., Kohl, M., Lekeux, P., 1999. Near infrared spectroscopy in large animals: optical pathlength and influence of hair covering and epidermal pigmentation. Vet. J. 158 (1), 48–52. doi:10.1053/tvjl.1998.0306.

Quaresima, V., Ferrari, M., 2016. Functional near-infrared spectroscopy (*f*NIRS) for assessing cerebral cortex function during human behavior in natural/social situations: a concise review. Org. Res. Methods 22 (1), 1–23. doi:10.1177/1094428116658959.

Rao, S.M., Harrington, D.L., Haaland, K.Y., Bobholz, J.A., Cox, R.W., Binder, J.R., 1997. Distributed neural systems underlying the timing of movements. J. Neurosci. 17 (14), 5528–5535. doi:10.1523/JNEUROSCI.17-14-05528.1997.

Repp, B.H., 2005. Sensorimotor synchronization: a review of the tapping literature. Psychon. Bull. Rev. 12 (6), 969–992. doi:10.3758/BF03206433.

Rubia, K., Smith, A., 2004. The neural correlates of cognitive time management: a review.. Acta Neurobiologiae Experimentalis 64 (3), 329–340.

Sato, T., Ito, M., Suto, T., Kameyama, M., Suda, M., Yamagishi, Y., Ohshima, A., Uehara, T., Fukuda, M., Mikuni, M., 2007. Time courses of brain activation and their implications for function: a multichannel near-infrared spectroscopy study during finger tapping. Neurosci. Res. 58 (3), 297–304. doi:10.1016/j.neures.2007.03.014.

Schmidt, R.A., Lee, T.D., Winstein, C., Wulf, G., Zelaznik, H.N., 1988. Motor Control and Learning: a Behavioral Emphasis, 6 Human Kinetics.

Scholkmann, F., Hafner, T., Metz, A.J., Wolf, M., Wolf, U., 2017. Effect of short-term colored-light exposure on cerebral hemodynamics and oxygenation, and systemic physiological activity. Neurophotonics 4 (4). doi:10.1117/1.NPh.4.4.045005. Article e045005

Scholkmann, F., Kleiser, S., Metz, A.J., Zimmermann, R., Pavia, J.M., Wolf, U., Wolf, M., 2014. A review on continuous wave functional near-infrared spectroscopy and imaging instrumentation and methodology. NeuroImage 85, 6–27. doi:10.1016/j.neuroimage.2013.05.004.

Schubotz, R.I., Friederici, A.D., von Cramon, D.Y., 2000. Time perception and motor timing: a common cortical and subcortical basis revealed by *f*MRI. NeuroImage 11 (1), 1–12. doi:10.1006/nimg.1999.0514.

Shadgan, B., Molavi, B., Reid, W.D., Dumont, G., Macnab, A.J., 2010. Do radio frequencies of medical instruments common in the operating room interfere with near-infrared spectroscopy signals?, pp. 1–6. doi:10.1117/12.842712.

Simonsohn, U., 2015. Small telescopes: detectability and the evaluation of replication results. Psychol. Sci. 26 (5), 559–569. doi:10.1177/0956797614567341.

Strangman, G., Boas, D.A., Sutton, J.P., 2002. Non-invasive neuroimaging using near-infrared light. Biol. Psychiatry 52 (7), 679–693. doi:10.1016/S0006-3223(02)01550-0.

Tachtsidis, I., Elwell, C.E., Leung, T.S., Lee, C.-W., Smith, M., Delpy, D.T., 2004. Investigation of cerebral haemodynamics by near-infrared spectroscopy in young healthy volunteers reveals posture-dependent spontaneous oscillations. Physiol. Meas. 25 (2), 437–445. doi:10.1088/0967-3334/25/2/003.

Tachtsidis, I., Scholkmann, F., 2016. False positives and false negatives in functional near-infrared spectroscopy: Issues, challenges, and the way forward. Neurophotonics 3 (3). doi:10.1117/1.NPh.3.3.031405. Article e031405

Treisman, M., 1963. Temporal discrimination and the indifference interval: Implications for a model of the "internal clock".. Psychol. Monogr.: Gen. Appl. 77 (13), 1–31. doi:10.1037/h0093864.

Vergotte, G., Perrey, S., Muthuraman, M., Janaqi, S., Torre, K., 2018. Concurrent changes of brain functional connectivity and motor variability when adapting to task constraints. Front. Physiol. 9. doi:10.3389/fphys.2018.00909. Article e909

Vergotte, G., Torre, K., Chirumamilla, V.C., Anwar, A.R., Groppa, S., Perrey, S., Muthuraman, M., 2017. Dynamics of the human brain network revealed by time-frequency effective connectivity in *f*NIRS. Biomed. Opt. Express 8 (11), 5326–5341. doi:10.1364/BOE.8.005326.

Williams, B.R., Ponesse, J.S., Schachar, R.J., Logan, G.D., Tannock, R., 1999. Development of inhibitory control across the life span. Dev. Psychol. 35 (1), 205–213.

Wilson, T.W., Kurz, M.J., Arpin, D.J., 2014. Functional specialization within the supplementary motor area: a *f*NIRS study of bimanual coordination. NeuroImage 85 (1), 445–450. doi:10.1016/j.neuroimage.2013.04.112.

Zelaznik, H.N., Spencer, R., Ivry, R.B., 2002. Dissociation of explicit and implicit timing in repetitive tapping and drawing movements.. J. Exp. Psychol.: Hum. Percept. Perform. 28 (3), 575. doi:10.1037/0096-1523.28.3.575.